Bumps in simple two-dimensional neural field models

Olivier Faugeras, François Grimbert

INSTITUT NATIONAL DE RECHERCHE EN INFORMATIQUE ET EN AUTOMATIQUE

Bumps in simple two-dimensional neural field models

Olivier Faugeras — François Grimbert

N° ????

December 2007

Thème BIO

Rapport de recherche

ISSN 0249-6399 ISRN INRIA/RR--????--FR+ENG

Bumps in simple two-dimensional neural field models

Olivier Faugeras*, François Grimbert*

Thème BIO — Systèmes biologiques
Projet Odyssée

Rapport de recherche n° ???? — December 2007 — 19 pages

Abstract: *Neural field* models first appeared in the 50's, but the theory really took off in the 70's with the works of Wilson and Cowan [11, 12] and Amari [2, 1]. Neural fields are continuous networks of interacting neural masses, describing the dynamics of the cortical tissue at the population level. In this report, we study homogeneous stationary solutions (i.e independent of the spatial variable) and bump stationary solutions (i.e. localized areas of high activity) in two kinds of infinite two-dimensional neural field models composed of two neuronal layers (excitatory and inhibitory neurons). We particularly focus on bump patterns, which have been observed in the prefrontal cortex and are involved in working memory tasks [9]. We first show how to derive neural field equations from the spatialization of mesoscopic cortical column models. Then, we introduce classical techniques borrowed from Coombes [3] and Folias and Bressloff [7] to express bump solutions in a closed form and make their stability analysis. Finally we instantiate these techniques to construct stable two-dimensional bump solutions.

Key-words: neural fields, neural masses, bumps, prefrontal cortex, linear stability analysis

This work was partially supported by Elekta AB.

* Projet Odyssée, INRIA Sophia-Antipolis

Unité de recherche INRIA Sophia Antipolis
2004, route des Lucioles, BP 93, 06902 Sophia Antipolis Cedex (France)
Téléphone : +33 4 92 38 77 77 — Télécopie : +33 4 92 38 77 65

Activités localisées dans des modèles simples de champs neuronaux

Résumé : Les modèles de champs neuronaux sont apparus dans les années cinquante, mais la théorie n'a véritablement pris son essor que dans les années soixante-dix avec les travaux de Wilson et Cowan [11, 12] et Amari [2, 1]. Les champs neuronaux sont des réseaux continus de masses neuronales interconnectées qui décrivent la dynamique du tissu cortical à l'échelle des populations de neurones. Dans ce rapport, nous étudions les solutions stationaires homogènes (indépendantes de la variable d'espace) et celles en forme de bosses (correspondant à des zones localisées de forte activité) dans deux types de modèles de champs neuronaux à deux dimensions comportant deux couches neuronales (neurones excitateurs et inhibiteurs). Nous nous concentrons particulièrement sur les bosses, qui ont été observées dans le cortex préfrontal et sont impliquées dans les mécanismes de la mémoire de travail [9]. Dans un premier temps, nous montrons comment obtenir les équations de champs neuronal par simple spatialisation de modèles mésoscopiques de colonnes corticales. Ensuite, nous présentons des techniques classiques employées par Coombes [3] et Folias et Bressloff [7] pour exprimer les bosses par une formule explicite et faire l'analyse de leur stabilité linéaire. Enfin, nous instancions ces techniques pour construire des bosses stables à deux dimensions.

Mots-clés : champs neuronaux, masses neuronales, bosses, cortex préfrontal, stabilité linéaire

Contents

We consider the formation of bumps in an infinite two-dimensional neural field composed of two interacting layers of neural masses: excitatory and inhibitory masses such as shown in figure 1. Each point of the field can be viewed as a cortical column composed of two neural masses (one in each layer). Columns are assembled spatially to form the neural field, which is meant to represent a macroscopic part of the neocortex, e.g. a cortical area.

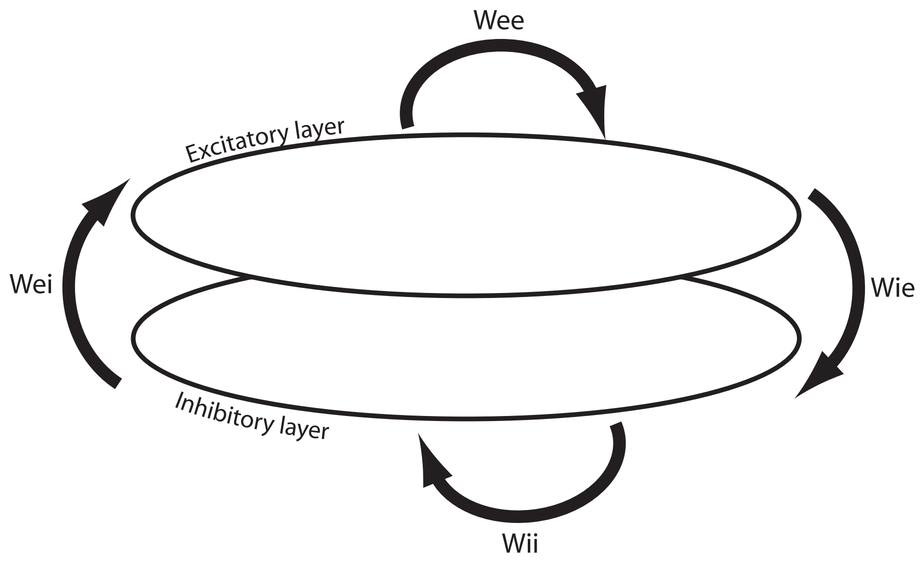

Figure 1: *Two interacting neuronal layers of excitatory and inhibitory cells.*

In this report, we consider an infinite neural field. Then each layer can be identified with $\mathbb{R}^2$. Neural masses are characterized by their layer, e or i, and their horizontal coordinates $\mathbf{r} = (r_1, r_2)$.

1 Neural field equations

1.1 Interactions between a few neural masses

The following derivation is built after Ermentrout's review [5]. We consider n interacting neural masses. Each mass k is described by its membrane potential $V_k(t)$ or by its instantaneous firing rate $\nu_k(t)$, the relation between the two quantities being of the form $\nu_k(t) = S_k(V_k(t))$ [8, 4], where S_k is sigmoidal and depends on the layer of neuron k. Here we consider the limiting case of a Heaviside function

$$S_x(V) = \overline{\nu}_x \, H(V - \theta_x), \quad x \in \{e, i\},$$

where H is the Heaviside distribution, $\overline{\nu}_x$ the maximal firing rate of neurons of type x and θ_x their excitabillity threshold.

The mass m is connected to the mass k. A single action potential from m is seen as a post-synaptic potential $PSP_{km}(t-s)$ by k, where s is the time of the spike hitting the terminal and t the time after the spike. We neglect the delays due to the distance travelled down the axon by the spikes. Assuming that the post-synaptic potentials sum linearly, the membrane potential of the mass k is

$$V_k(t) = \sum_{m,p} PSP_{km}(t - t_p)$$

where the sum is taken over presynaptic masses and the arrival times of the spikes produced by them. The number of spikes arriving between t and $t + dt$ is $\nu_m(t)dt$. Therefore we have

$$V_k(t) = \sum_m \int_{t_0}^{t} PSP_{km}(t-s)\nu_m(s)\,ds = \sum_m \int_{t_0}^{t} PSP_{km}(t-s)S_m(V_m(s))\,ds,$$

or, equivalently

$$\nu_k(t) = S_k\left(\sum_m \int_{t_0}^{t} PSP_{km}(t-s)\nu_m(s)\,ds\right) \tag{1}$$

There are two main simplifying assumptions that appear in the literature [5] and yield two different models.

1.1.1 The voltage-based model

The assumption, made in [10], is that the post-synaptic potential has the same shape no matter which presynaptic neuron type caused it, the sign and amplitude may vary though. This leads to the relation

$$PSP_{km}(t) = W_{km} PSP_k(t).$$

If $W_{km} > 0$ mass m excites mass k whereas it inhibits it when $W_{km} < 0$. Finally, if we assume that $PSP_{km}(t) = W_{km} e^{-t/\tau_k} H(t)$ (where H is the Heaviside distribution), or equivalently that

$$\tau_k \frac{dPSP_{km}(t)}{dt} + PSP_{km}(t) = W_{km}\tau_k \delta(t), \tag{2}$$

we end up with the following system of ordinary differential equations

$$\frac{dV_k(t)}{dt} + \frac{V_k(t)}{\tau_k} = \sum_m W_{km} S_m(V_m(t)) + I_k^{\text{ext}}(t), \quad k = 1, ..., n, \tag{3}$$

that describes the dynamic behaviour of the network. We have added an external current $I_k^{\text{ext}}(t) \geq 0$ to model external input to mass k. We introduce the $n \times n$ matrix $\mathbf{W} = W_{km}$, and the function $\mathbf{S} : \mathbb{R}^n \to \mathbb{R}^n$ such that $\mathbf{S}(\mathbf{x})$ is the vector of coordinates $S_k(x_k)$. We rewrite (3) in vector form and obtain the following system of n ordinary differential equations

$$\dot{\mathbf{V}} = -\mathbf{L}\mathbf{V} + \mathbf{W}\mathbf{S}(\mathbf{V}) + \mathbf{I}^{\text{ext}}, \tag{4}$$

where $\mathbf{L}$ is the diagonal matrix $\mathbf{L} = \mathrm{diag}(1/\tau_\mathrm{k})$.

1.1.2 The activity-based model

The assumption is that the shape of a post-synaptic potential depends only on the nature of the presynaptic mass, that is

$$PSP_{km}(t) = W_{km} PSP_m(t).$$

As above we suppose that $PSP_{km}(t)$ satisfies the differential equation (2) and define the activity to be

$$A_m(t) = \int_{t_0}^{t} PSP_m(t-s)\nu_m(s)\, ds.$$

A similar derivation yields the following set of ordinary differential equations

$$\frac{dA_k(t)}{dt} + \frac{A_k(t)}{\tau_k} = S_k\left(\sum_m W_{km} A_m(t) + I_k^{\mathrm{ext}}(t)\right), \quad k = 1, ..., n.$$

We rewrite this in vector form

$$\dot{\mathbf{A}} = -\mathbf{L}\mathbf{A} + \mathbf{S}(\mathbf{W}\mathbf{A} + \mathbf{I}^{\mathrm{ext}}). \tag{5}$$

1.2 Neural fields models

Following the above rules for a discrete network of masses, we form a two layers continuum of masses.

We note $\mathbf{V}(\mathbf{r}, t)$ (respectively $\mathbf{A}(\mathbf{r}, t)$) the 2-dimensional state vector at the point $\mathbf{r}$ of the continuum and at time t. We introduce the 2×2 matrix function $\mathbf{W}(\mathbf{r},\, \mathbf{r}')$ which describes how the mass at point $\mathbf{r}'$ influences that at point $\mathbf{r}$. More precisely, $W_{xy}(\mathbf{r}, \mathbf{r}')$ describes how the mass in layer y at point $\mathbf{r}'$ influences the mass in layer x at point $\mathbf{r}$. We call $\mathbf{W}$ the connectivity matrix function. Equation (4) can now be extended to

$$\dot{\mathbf{V}}(\mathbf{r}, t) = -\mathbf{L}\mathbf{V}(\mathbf{r}, t) + \int_{\mathbb{R}^2} \mathbf{W}(\mathbf{r}, \mathbf{r}')\mathbf{S}(\mathbf{V}(\mathbf{r}', t))\, d\mathbf{r}' + \mathbf{I}^{\mathrm{ext}}(\mathbf{r}, t), \tag{6}$$

and equation (5) to

$$\dot{\mathbf{A}}(\mathbf{r}, t) = -\mathbf{L}\mathbf{A}(\mathbf{r}, t) + \mathbf{S}\left(\int_{\mathbb{R}^2} \mathbf{W}(\mathbf{r}, \mathbf{r}')\mathbf{A}(\mathbf{r}', t)\, d\mathbf{r}' + \mathbf{I}^{\mathrm{ext}}(\mathbf{r}, t)\right). \tag{7}$$

In detail, we have the following systems

$$\left\{\begin{array}{l} \dot{V}_e(\mathbf{r}, t) + \frac{V_e(\mathbf{r}, t)}{\tau_e} = \int_{\mathbb{R}^2} W_{ee}(\mathbf{r}, \mathbf{r}')S_e(V_e(\mathbf{r}', t)) + W_{ei}(\mathbf{r}, \mathbf{r}')S_i(V_i(\mathbf{r}', t))\, d\mathbf{r}' + I_e^{\mathrm{ext}}(\mathbf{r}, t) \\ \dot{V}_i(\mathbf{r}, t) + \frac{V_i(\mathbf{r}, t)}{\tau_i} = \int_{\mathbb{R}^2} W_{ie}(\mathbf{r}, \mathbf{r}')S_e(V_e(\mathbf{r}', t)) + W_{ii}(\mathbf{r}, \mathbf{r}')S_i(V_i(\mathbf{r}', t))\, d\mathbf{r}' + I_i^{\mathrm{ext}}(\mathbf{r}, t) \end{array}\right. , \tag{8}$$

and

$$\left\{\begin{array}{l} \dot{A}_e(\mathbf{r}, t) + \frac{A_e(\mathbf{r}, t)}{\tau_e} = S_e\left(\int_{\mathbb{R}^2} W_{ee}(\mathbf{r}, \mathbf{r}')A_e(\mathbf{r}', t) + W_{ei}(\mathbf{r}, \mathbf{r}')A_i(\mathbf{r}', t)\, d\mathbf{r}' + I_e^{\mathrm{ext}}(\mathbf{r}, t)\right) \\ \dot{A}_i(\mathbf{r}, t) + \frac{A_i(\mathbf{r}, t)}{\tau_i} = S_i\left(\int_{\mathbb{R}^2} W_{ie}(\mathbf{r}, \mathbf{r}')A_e(\mathbf{r}', t) + W_{ii}(\mathbf{r}, \mathbf{r}')A_i(\mathbf{r}', t)\, d\mathbf{r}' + I_i^{\mathrm{ext}}(\mathbf{r}, t)\right) \end{array}\right. . \tag{9}$$

In this study we will consider $\mathbf{W}$ translation invariant, $\mathbf{W}(\mathbf{r}, \mathbf{r}') = \mathbf{W}(\mathbf{r} - \mathbf{r}')$.

2 Study of bump solutions

This is an extension of the work of Stephen Coombes [3].

2.1 Stationary solutions

We look for stationary solutions of the systems (8) and (9):

$$\begin{cases} v_e(\mathbf{r}) = \tau_e \int_{\mathbb{R}^2} W_{ee}(\mathbf{r}-\mathbf{r}')S_e(v_e(\mathbf{r}')) + W_{ei}(\mathbf{r}-\mathbf{r}')S_i(v_i(\mathbf{r}'))\,d\mathbf{r}' + \tau_e\, I_e^{\mathrm{ext}}(\mathbf{r}) \\ v_i(\mathbf{r}) = \tau_i \int_{\mathbb{R}^2} W_{ie}(\mathbf{r}-\mathbf{r}')S_e(v_e(\mathbf{r}')) + W_{ii}(\mathbf{r}-\mathbf{r}')S_i(v_i(\mathbf{r}'))\,d\mathbf{r}' + \tau_i\, I_i^{\mathrm{ext}}(\mathbf{r}) \end{cases} \tag{10}$$

and

$$\begin{cases} a_e(\mathbf{r}) = \tau_e\, S_e\left(\int_{\mathbb{R}^2} W_{ee}(\mathbf{r}-\mathbf{r}')a_e(\mathbf{r}') + W_{ei}(\mathbf{r}-\mathbf{r}')a_i(\mathbf{r}')\,d\mathbf{r}' + I_e^{\mathrm{ext}}(\mathbf{r})\right) \\ a_i(\mathbf{r}) = \tau_i\, S_i\left(\int_{\mathbb{R}^2} W_{ie}(\mathbf{r}-\mathbf{r}')a_e(\mathbf{r}') + W_{ii}(\mathbf{r}-\mathbf{r}')a_i(\mathbf{r}')\,d\mathbf{r}' + I_i^{\mathrm{ext}}(\mathbf{r})\right) \end{cases} . \tag{11}$$

We introduce the terms $\widehat{W}_{xy} = \int_{\mathbb{R}^2} W_{xy}(\mathbf{r})\,d\mathbf{r}$.

2.1.1 Homogeneous solutions

Homogeneous stationary solutions (i.e., independent of the space variable) verify the systems

$$\begin{cases} v_e = \tau_e\, \left(\widehat{W}_{ee}S_e(v_e) + \widehat{W}_{ei}S_i(v_i) + I_e^{\mathrm{ext}}\right) \\ v_i = \tau_i\, \left(\widehat{W}_{ie}S_e(v_e) + \widehat{W}_{ii}S_i(v_i) + I_i^{\mathrm{ext}}\right) \end{cases} \tag{12}$$

and

$$\begin{cases} a_e = \tau_e\, S_e\left(\widehat{W}_{ee}a_e + \widehat{W}_{ei}a_i + I_e^{\mathrm{ext}}(\mathbf{r})\right) \\ a_i = \tau_i\, S_i\left(\widehat{W}_{ie}a_e + \widehat{W}_{ii}a_i + I_i^{\mathrm{ext}}(\mathbf{r})\right) \end{cases} . \tag{13}$$

These systems have at most four solutions. In the case of (12), (v_e, v_i) possibly have four values because there are two possible values for each $S_x(v_x)$ (namely, 0 and $\overline{\nu}_x$), depending on whether v_e and v_i are below or above the thresholds θ_e and θ_i. We obtain two expressions, for v_e and v_i, and they have to satisfy the threshold conditions, depending on $\widehat{\mathbf{W}}$, $\mathbf{I}^{\mathrm{ext}}$ and τ_x, to be validated as actual solutions. In detail, the four possible solutions, with their threshold conditions are

$$\begin{cases} v_e = \tau_e\, I_e^{\mathrm{ext}} \leq \theta_e \\ v_i = \tau_i\, I_i^{\mathrm{ext}} \leq \theta_i \end{cases} \tag{14}$$

$$\begin{cases} v_e = \tau_e\, \widehat{W}_{ee}\, \overline{\nu}_e + \tau_e\, I_e^{\mathrm{ext}} \geq \theta_e \\ v_i = \tau_i\, \widehat{W}_{ie}\, \overline{\nu}_e + \tau_i\, I_i^{\mathrm{ext}} \leq \theta_i \end{cases} \tag{15}$$

$$\begin{cases} v_e = \tau_e\, \widehat{W}_{ei}\, \overline{\nu}_i + \tau_e\, I_e^{\mathrm{ext}} \leq \theta_e \\ v_i = \tau_i\, \widehat{W}_{ii}\, \overline{\nu}_i + \tau_i\, I_i^{\mathrm{ext}} \geq \theta_i \end{cases} \tag{16}$$

$$\begin{cases} v_e = \tau_e \left(\widehat{W}_{ee}\, \overline{\nu}_e + \widehat{W}_{ei}\, \overline{\nu}_i + I_e^{\text{ext}} \right) \geq \theta_e \\ v_i = \tau_i \left(\widehat{W}_{ie}\, \overline{\nu}_e + \widehat{W}_{ii}\, \overline{\nu}_i + I_i^{\text{ext}} \right) \geq \theta_i \end{cases} \tag{17}$$

One can easily see that some of these pairs of threshold conditions are mutually exclusive, namely (14) and (16), (15) and (16), and (15) and (17). Since in three pairs of solutions, at least two of them will be incompatible, there can be at most two homogeneous stationary solutions. The case of zero solutions is impossible because it would require two mutually exclusive conditions like $\tau_e\, I_e^{\text{ext}} > \theta_e$ and $\tau_e\, \widehat{W}_{ee}\, \overline{\nu}_e + \tau_e\, I_e^{\text{ext}} < \theta_e$. Hence, one and two solutions are the only possible scenarii and both can actually occur. For example, (14) and (15) are compatible, but if $\tau_e\, I_e^{\text{ext}} > \theta_e$, only (15) remains true.

In the case of (13), we assign a value to each a_x (0 or $\tau_x \overline{\nu}_x$) and impose that the term inside each S_x verifies the corresponding threshold condition. We can derive a similar discussion as above and prove that this system can only have one or two solutions. Remark that in this second case, the input needs not to be homogeneous.

2.1.2 Circularly symmetric bumps solutions

Looking for bump solutions means that we pay special attention to the domain of the field where the components of $\mathbf{v}$ or $\mathbf{a}$ are "high". Indeed, bumps can be defined as localized high activity areas on the neural field. Here "high activity" means that the terms in the sigmoids are above the characteristic thresholds. We look at rotationally invariant (i.e. depending only on $r = \|\mathbf{r}\|$) stationary solutions centered at the origin of $\mathbb{R}^2$. It is not difficult to check on systems (10) and (11) that this only makes sense for $\mathbf{I}^{\text{ext}}$ and $\mathbf{W}$ rotationally invariant.
We look for bump solutions so that S_e and S_i are on a high state only in the disks D_{r_e} and D_{r_i}, of radii r_e and r_i respectively. If we define

$$b_{xy}(r, \rho) = \overline{\nu}_y \int_{D_\rho} W_{xy}(|\mathbf{r} - \mathbf{r}'|)\, d\mathbf{r}',$$

these bumps necessarily verify

$$\begin{cases} v_e(r) = \tau_e\ \left(b_{ee}(r, r_e) + b_{ei}(r, r_i) + I_e^{\text{ext}}(r)\right) \\ v_i(r) = \tau_i\ \left(b_{ie}(r, r_e) + b_{ii}(r, r_i) + I_i^{\text{ext}}(r)\right) \end{cases} \tag{18}$$

and

$$\begin{cases} a_e(r) = \tau_e\, S_e\left(\tau_e b_{ee}(r, r_e) + \tau_i b_{ei}(r, r_i) + I_e^{\text{ext}}(r)\right) \\ a_i(r) = \tau_i\, S_i\left(\tau_e b_{ie}(r, r_e) + \tau_i b_{ii}(r, r_i) + I_i^{\text{ext}}(r)\right) \end{cases} . \tag{19}$$

At this point, it looks like we have an explicit formula for the bumps in the voltage-based and the activity-based frameworks. It is not true, since for a general (r_e, r_i) the corresponding solution may not be consistent with the threshold conditions, which for the voltage case amount to

$$\begin{cases} \tau_e\ \left(b_{ee}(r, r_e) + b_{ei}(r, r_i) + I_e^{\text{ext}}(r)\right) > \theta_e,\ \text{iff}\ r < r_e \\ \tau_i\ \left(b_{ie}(r, r_e) + b_{ii}(r, r_i) + I_i^{\text{ext}}(r)\right) > \theta_i,\ \text{iff}\ r < r_i \end{cases} , \tag{20}$$

and for the activity case to

$$\begin{cases} \tau_e b_{ee}(r,r_e) + \tau_i b_{ei}(r,r_i) + I_e^{\text{ext}}(r) > \theta_e, \text{ iff } r < r_e \\ \tau_e b_{ie}(r,r_e) + \tau_i b_{ii}(r,r_i) + I_i^{\text{ext}}(r) > \theta_i, \text{ iff } r < r_i \end{cases}. \tag{21}$$

So, to solve the bumps existence problems, one has to find r_e and r_i such that the (necessary and) sufficient condition (20) or (21) is satisfied. We will refer to expressions (18) and (19) as *pseudo-bumps*.
As in [3] , we can rewrite $\mathbf{b}$ using Bessel functions. The Hankel transform of $W(r)$ is defined by

$$\widetilde{W}(k) = \int_0^\infty W(r) J_0(kr) r\, dr,$$

where J_ν is the Bessel function of the first kind of order ν, and we have the following property

$$\widetilde{W}(k) = \int_{\mathbb{R}^2} e^{i\mathbf{k}.\mathbf{r}} W(\mathbf{r})\, d\mathbf{r},$$

where we have considered the rotationally invariant 2D function $W(\mathbf{r}) = W(r)$. Then, we can write

$$W(r) = \int_0^\infty \widetilde{W}(k) J_0(rk) k\, dk.$$

According to [7], we obtain

$$\int_{D_\rho} W(|\mathbf{r}-\mathbf{r}'|)\, d\mathbf{r}' = 2\pi\rho \int_0^\infty \widetilde{W}(k) J_0(rk) J_1(\rho k)\, dk.$$

Then we can use the properties of Bessel functions. For example, we can get rid of integrals in the expression of the bumps with appropriate connectivity kernels. In [3] the author considers the following approximation

$$e^{-r} \approx \frac{4}{3}(K_0(r) - K_0(2r)),$$

where K_ν is the modified Bessel function of the second type of order ν, and exploit the fact that the Hankel transform of $K_0(pr)$ is equal to $H_p(k) = (k^2+p^2)^{-1}$. So, if we choose to approximate exponential connectivities of the form

$$\begin{cases} W_{ee}(r) = c_{ee} e^{-\delta_e r} & W_{ie}(r) = c_{ie} e^{-\delta_e r} \\ W_{ei}(r) = c_{ei} e^{-\delta_i r} & W_{ii}(r) = c_{ii} e^{-\delta_i r} \end{cases},$$

we have

$$\begin{aligned} \widetilde{W}_{ee}(k) &= \tfrac{4}{3} c_{ee} \left(\frac{1}{k^2+\delta_e^2} - \frac{1}{k^2+4\delta_e^2} \right) \\ \widetilde{W}_{ei}(k) &= \tfrac{4}{3} c_{ei} \left(\frac{1}{k^2+\delta_i^2} - \frac{1}{k^2+4\delta_i^2} \right) \\ \widetilde{W}_{ie}(k) &= \tfrac{4}{3} c_{ie} \left(\frac{1}{k^2+\delta_e^2} - \frac{1}{k^2+4\delta_e^2} \right) \\ \widetilde{W}_{ii}(k) &= \tfrac{4}{3} c_{ii} \left(\frac{1}{k^2+\delta_i^2} - \frac{1}{k^2+4\delta_i^2} \right) \end{aligned}, \tag{22}$$

and use the following property to obtain the explicit formula for the bumps

$$\int_0^{+\infty} H_x(k) J_0(rk) J_1(\rho k)\, dk = \begin{cases} \frac{1}{x} I_1(x\rho) K_0(xr) & r \geq \rho \\ \frac{1}{x^2 \rho} - \frac{1}{x} I_0(xr) K_1(x\rho) & r < \rho \end{cases},$$

where I_ν is the modified Bessel function of the first type of order ν. Hence, we get

$$b_{xy}(r,\rho) = \frac{8}{3}\,\pi\,\frac{\overline{\nu}_y}{\delta_y}\,c_{xy}\,\rho \begin{cases} I_1(\delta_y \rho) K_0(\delta_y r) - \frac{1}{2} I_1(2\delta_y \rho) K_0(2\delta_y r) & r \geq \rho \\ \frac{3}{4\delta_y \rho} - I_0(\delta_y r) K_1(\delta_y \rho) + \frac{1}{2} I_0(2\delta_y r) K_1(2\delta_y \rho) & r < \rho \end{cases}. \quad (23)$$

This thus provide an expression for the pseudo-bumps (18) and (19) explicitly depending only on r.

In these developments we have seen how crucial is the choice of the connectivity kernels to make bumps calculations tractable.

2.2 Stability of the solutions

2.2.1 Homogeneous solutions

We make a linear stability analysis of the homogeneous solutions $\mathbf{v}$ of the system (8). We consider perturbations of the form

$$\mathbf{V}(\mathbf{r}, t) = \mathbf{v} + \boldsymbol{\phi}(\mathbf{r}) e^{\lambda t}$$

with $|\boldsymbol{\phi}| \ll |\mathbf{v}|$, inject them in the corresponding linearized equation, and simplify the exponential terms. We have therefore

$$(\lambda \mathrm{Id} + \mathbf{L})\boldsymbol{\phi}(\mathbf{r}) = \int_{\mathbb{R}^2} \mathbf{W}(|\mathbf{r} - \mathbf{r}'|)\, D\mathbf{S}(\mathbf{v}) \boldsymbol{\phi}(\mathbf{r}')\, d\mathbf{r}',$$

and since $D\mathbf{S}(\mathbf{v}) = 0$, we obtain

$$(\lambda \mathrm{Id} + \mathbf{L})\boldsymbol{\phi}(\mathbf{r}) = 0,$$

which has two negative solutions $\lambda = -\frac{1}{\tau_e}$ and $\lambda = -\frac{1}{\tau_i}$.
Hence, the homogeneous solutions are stable. A similar derivation guarantees the stability of the homogeneous solutions in the activity case.

2.2.2 Bump solutions

Here we make a linear stability analysis of the bumps solutions $\mathbf{v}(r)$ and $\mathbf{a}(r)$ of systems (8) and (9). We consider perturbations of the form

$$\mathbf{V}(\mathbf{r}, t) = \mathbf{v}(r) + \boldsymbol{\phi}(\mathbf{r}) e^{\lambda t} \quad \text{and} \quad \mathbf{A}(\mathbf{r}, t) = \mathbf{a}(r) + \boldsymbol{\psi}(\mathbf{r}) e^{\lambda t},$$

with $|\boldsymbol{\phi}| \ll |\mathbf{v}|$ and $|\boldsymbol{\psi}| \ll |\mathbf{a}|$, inject them in their corresponding linearized equations, and simplify the exponential terms. We obtain

$$(\lambda \mathrm{Id} + \mathbf{L})\boldsymbol{\phi}(\mathbf{r}) = \int_{\mathbb{R}^2} \mathbf{W}(|\mathbf{r}-\mathbf{r}'|)\, D\mathbf{S}(\mathbf{v}(r'))\boldsymbol{\phi}(\mathbf{r}')\, d\mathbf{r}'$$

and

$$(\lambda \mathrm{Id} + \mathbf{L})\boldsymbol{\phi}(\mathbf{r}) = D\mathbf{S}\left(\int_{\mathbb{R}^2} \mathbf{W}(|\mathbf{r}-\mathbf{r}'|)\, \mathbf{a}(r')\, d\mathbf{r}' + \mathbf{I}^{\mathrm{ext}}(r)\right)\int_{\mathbb{R}^2} \mathbf{W}(|\mathbf{r}-\mathbf{r}'|)\, \boldsymbol{\phi}(\mathbf{r}')\, d\mathbf{r}'.$$

We will use the fact that

$$D\mathbf{S}(\mathbf{f}(r)) = \begin{bmatrix} \dfrac{\delta(r-r_e)}{|f_e'(r_e)|} & 0 \\ 0 & \dfrac{\delta(r-r_i)}{|f_i'(r_i)|} \end{bmatrix},$$

where functions f_xs only reach θ_x at r_x.
In the voltage case, we obtain

$$\begin{array}{rcl} \lambda_e\phi_e(\mathbf{r}) & = & \alpha_e \int_0^{2\pi} W_{ee}(|\mathbf{r}-\mathbf{r}_e'|)\, \phi_e(\mathbf{r}_e')\, d\theta' + \alpha_i \int_0^{2\pi} W_{ei}(|\mathbf{r}-\mathbf{r}_i'|)\, \phi_i(\mathbf{r}_i')\, d\theta' \\ \lambda_i\phi_i(\mathbf{r}) & = & \alpha_e \int_0^{2\pi} W_{ie}(|\mathbf{r}-\mathbf{r}_e'|)\, \phi_e(\mathbf{r}_e')\, d\theta' + \alpha_i \int_0^{2\pi} W_{ii}(|\mathbf{r}-\mathbf{r}_i'|)\, \phi_i(\mathbf{r}_i')\, d\theta' \end{array}, \tag{24}$$

where $\mathbf{r}_x' = [r_x, \theta']^T$, and

$$\lambda_x = \lambda + \frac{1}{\tau_x}, \quad \alpha_x = \frac{r_x}{|v_x'(r_x)|}.$$

In the activity case, we have

$$\begin{array}{rcl} \lambda_e\psi_e(\mathbf{r}) & = & \beta_e/r_e\, \delta(r-r_e) \int_{\mathbb{R}^2} W_{ee}(|\mathbf{r}-\mathbf{r}'|)\, \psi_e(\mathbf{r}') + W_{ei}(|\mathbf{r}-\mathbf{r}'|)\, \psi_i(\mathbf{r}')\, d\mathbf{r}' \\ \lambda_i\psi_i(\mathbf{r}) & = & \beta_i/r_i\, \delta(r-r_i) \int_{\mathbb{R}^2} W_{ie}(|\mathbf{r}-\mathbf{r}'|)\, \psi_e(\mathbf{r}') + W_{ii}(|\mathbf{r}-\mathbf{r}'|)\, \psi_i(\mathbf{r}')\, d\mathbf{r}' \end{array},$$

where

$$\beta_x = \frac{r_x}{|(\tau_e b_{xe}'(r_x, r_e) + \tau_i b_{xi}'(r_x, r_i)) + I_x^{\mathrm{ext}\prime}(r_x)|}.$$

We see that the mass of distributions ψ_e and ψ_i is concentrated on the circles $\{r = r_e\}$ and $\{r = r_i\}$ respectively because of the Dirac terms in the above formulas. So we can rewrite them as

$$\begin{array}{rcl} \lambda_e\psi_e(\mathbf{r}) & = & \beta_e/r_e\, \delta(r-r_e)\left(r_e \int_0^{2\pi} W_{ee}(|\mathbf{r}-\mathbf{r}_e'|)\, \psi_e(\mathbf{r}_e')\, d\theta' + r_i \int_0^{2\pi} W_{ei}(|\mathbf{r}-\mathbf{r}_i'|)\, \psi_i(\mathbf{r}_i')\, d\theta'\right) \\ \lambda_i\psi_i(\mathbf{r}) & = & \beta_i/r_i\, \delta(r-r_i)\left(r_e \int_0^{2\pi} W_{ie}(|\mathbf{r}-\mathbf{r}_e'|)\, \psi_e(\mathbf{r}_e')\, d\theta' + r_i \int_0^{2\pi} W_{ii}(|\mathbf{r}-\mathbf{r}_i'|)\, \psi_i(\mathbf{r}_i')\, d\theta'\right) \end{array}. \tag{25}$$

Separation of radial and angular variables

We specialize the perturbations by separating angular and radial variables

$$\boldsymbol{\zeta}^m(\mathbf{r}) = \boldsymbol{\zeta}^m(r)e^{im\theta}, \quad m \in \mathbb{Z},$$

with $\boldsymbol{\zeta} = \boldsymbol{\phi}$ or $\boldsymbol{\psi}$. By a change of variable $\varphi = \theta' - \theta$, we obtain

$$\int_0^{2\pi} W_{yx}(|\mathbf{r} - \mathbf{r}'_x|)\zeta_x^m(\mathbf{r}'_x)\, d\theta' = \zeta_x^m(r_x)e^{im\theta} \int_0^{2\pi} W_{yx}(|r - r_x e^{i\varphi}|)e^{im\varphi}\, d\varphi,$$

with $\boldsymbol{\zeta} = \boldsymbol{\phi}$ or $\boldsymbol{\psi}$, and set

$$h_{yx}^m(r) = \int_0^{2\pi} W_{yx}(|r - r_x e^{i\varphi}|)e^{im\varphi}\, d\varphi = \int_0^{2\pi} W_{yx}(\sqrt{r^2 + r_x^2 - 2rr_x \cos\varphi}) \cos(m\varphi)\, d\varphi.$$

Now, in the voltage case, equations (24) can be rewritten

$$\begin{array}{rcl} \lambda_e \phi_e^m(r) & = & \alpha_e \phi_e^m(r_e)\, h_{ee}^m(r) + \alpha_i \phi_i^m(r_i)\, h_{ei}^m(r) \\ \lambda_i \phi_i^m(r) & = & \alpha_e \phi_e^m(r_e)\, h_{ie}^m(r) + \alpha_i \phi_i^m(r_i)\, h_{ii}^m(r) \end{array}.$$

We evaluate these equations for respectively $r = r_e$ and $r = r_i$, and set

$$\mathbf{M}(m) = \begin{pmatrix} \alpha_e h_{ee}^m(r_e) & \alpha_i h_{ei}^m(r_e) \\ \alpha_e h_{ie}^m(r_i) & \alpha_i h_{ii}^m(r_i) \end{pmatrix}.$$

Then we have

$$\left(\mathbf{M}(m) - \begin{pmatrix} \lambda_e & 0 \\ 0 & \lambda_i \end{pmatrix}\right) \begin{pmatrix} \phi_e^m(r_e) \\ \phi_i^m(r_i) \end{pmatrix} = 0,$$

or equivalently (as soon as $\phi_e^m(r_e)$ or $\phi_i^m(r_i) \neq 0$)

$$\det(\mathbf{M}(m) - \mathbf{L} - \lambda \mathrm{Id}) = 0,$$

which is a second order polynomial in the variable λ.
System (24) is stable to a given perturbation (i.e. given m) if and only if both roots of the above second order polynomial have a negative real part. This condition is equivalent to

$$\det(\mathbf{M}(m) - \mathbf{L}) > 0 \quad \text{and} \quad \mathrm{tr}\,(\mathbf{M}(m) - \mathbf{L}) < 0. \tag{26}$$

For equations (25), the specialization of the perturbation gives

$$\begin{array}{rcl} \lambda_e \psi_e^m(r) & = & \beta_e / r_e\, \delta(r - r_e)\, (r_e \psi_e^m(r_e)\, h_{ee}^m(r) + r_i \psi_i^m(r_i)\, h_{ei}^m(r)) \\ \lambda_i \psi_i^m(r) & = & \beta_i / r_i\, \delta(r - r_i)\, (r_e \psi_e^m(r_e)\, h_{ie}^m(r) + r_i \psi_i^m(r_i)\, h_{ii}^m(r)) \end{array}.$$

We integrate these expressions on $\mathbb{R}^+$

$$\begin{array}{rcl} \lambda_e \psi_e^m(r_e) & = & \beta_e / r_e\, (r_e \psi_e^m(r_e)\, h_{ee}^m(r_e) + r_i \psi_i^m(r_i)\, h_{ei}^m(r_e)) \\ \lambda_i \psi_i^m(r_i) & = & \beta_i / r_i\, (r_e \psi_e^m(r_e)\, h_{ie}^m(r_i) + r_i \psi_i^m(r_i)\, h_{ii}^m(r_i)) \end{array},$$

and set

$$\mathbf{M}'(m) = \begin{pmatrix} \beta_e h_{ee}^m(r_e) & \frac{r_i}{r_e}\beta_i h_{ei}^m(r_e) \\ \frac{r_e}{r_i}\beta_e h_{ie}^m(r_i) & \beta_i h_{ii}^m(r_i) \end{pmatrix} \quad \text{and} \quad \mathbf{M}''(m) = \begin{pmatrix} \beta_e h_{ee}^m(r_e) & \beta_i h_{ei}^m(r_e) \\ \beta_e h_{ie}^m(r_i) & \beta_i h_{ii}^m(r_i) \end{pmatrix}.$$

Then the stability condition is

$$\det\left(\mathbf{M}'(m) - \mathbf{L}\right) > 0 \quad \text{and} \quad \operatorname{tr}\left(\mathbf{M}'(m) - \mathbf{L}\right) < 0, \tag{27}$$

which is equivalent to

$$\det\left(\mathbf{M}''(m) - \mathbf{L}\right) > 0 \quad \text{and} \quad \operatorname{tr}\left(\mathbf{M}''(m) - \mathbf{L}\right) < 0. \tag{28}$$

Hence we obtain the same condition as in the voltage case with β_xs instead of α_xs.

3 Construction of bump solutions

When the connections are weak, we see from (10) and (11) that

$$\mathbf{V} \to \mathbf{L}^{-1}\mathbf{I}^{\text{ext}} \quad \text{and} \quad \mathbf{A} \to \mathbf{L}^{-1}\mathbf{S}(\mathbf{I}^{\text{ext}}).$$

So the form of the stationary solution is similar to the input.
Moreover, the solution is stable because the equations become

$$\dot{\mathbf{V}} \approx -\mathbf{L}\mathbf{V} + \mathbf{I}^{\text{ext}} \quad \text{and} \quad \dot{\mathbf{A}} \approx -\mathbf{L}\mathbf{A} + \mathbf{S}(\mathbf{I}^{\text{ext}}),$$

and the corresponding eigenvalues are $\lambda = -\frac{1}{\tau_e}$ and $\lambda = -\frac{1}{\tau_i}$. Hence a stable bump solution is easily obtained by choosing a bump-shaped input.

From now on, we will look at another, more complex particular case: self-sustained states of localized high activity, corresponding to $\mathbf{I}^{\text{ext}} = 0$. Because of the similarities between the equations of the two cases for the existence and stability of bumps, we will focus on the voltage-case in the forthcoming derivations. We will consider continuous, integrable connectivity kernels with radially decreasing absolute value $|W_{xy}|'(r) < 0$. All illustrations and simulations will be performed with pseudo-bumps given by b_{xy}s of the form (23). The parameters we have used to produce them are shown in table 1.

Parameters	$\begin{pmatrix} c_{ee} & c_{ei} \\ c_{ie} & c_{ii} \end{pmatrix}$	(τ_e, τ_i)	(δ_e, δ_i)	$(\overline{\nu}_e, \overline{\nu}_i)$
Values	$\begin{pmatrix} 0.75\,\delta_e & -0.08\,\delta_i \\ 0.15\,\delta_e & -0.02\,\delta_i \end{pmatrix}$	$(0.01, 0.02)$	$(1, 2)$	$(1, 1)$

Table 1: *Parameters used in computations.*

3.1 Existence

Each pair $(r_e, r_i) \in {\mathbb{R}_+}^2$ defines a pseudo-bump by formula (18), but not all of these pseudo-bumps are actual bumps satisfying the threshold conditions. Our goal here is to identify subdomains of the (r_e, r_i) plane where real bumps can be found, and discuss the dependence of the solutions on the excitability thresholds θ_e and θ_i.
We first discuss the existence of putative bumps depending on the values of the excitability thresholds of the layers.
The difficulty for the fulfillment of the sufficient conditions of existence (20) resides in their global nature. So, we will first try to satisfy weaker, local criteria. A pair $(r_e, r_i) \in \mathbb{R}_+^2$ being given, the corresponding pseudo-bump must satisfy three necessary local conditions to be a real bump

$$\left\{ \begin{array}{ccc} v_x(0) & > & \theta_x \\ v_x(r_x) & = & \theta_x \\ v_x(+\infty) & < & \theta_x \end{array} \right., \text{ for } x \in \{e, i\}.$$

Since $v_x(+\infty) = 0$[1], we can rewrite them more specifically as

$$\left\{ \begin{array}{l} \theta_e = \tau_e \, (b_{ee}(r_e, r_e) + b_{ei}(r_e, r_i)) \\ \theta_i = \tau_i \, (b_{ie}(r_i, r_e) + b_{ii}(r_i, r_i)) \end{array} \right. \tag{29}$$

and

$$\left\{ \begin{array}{l} 0 \, < \, b_{ee}(r_e, r_e) + b_{ei}(r_e, r_i) \, < \, b_{ee}(0, r_e) + b_{ei}(0, r_i) \\ 0 \, < \, b_{ie}(r_i, r_e) + b_{ii}(r_i, r_i) \, < \, b_{ie}(0, r_e) + b_{ii}(0, r_i) \end{array} \right. . \tag{30}$$

In particular, given a pair of radii (r_e, r_i) (and hence a pseudo-bump), a unique pair of thresholds could satisfy the above conditions. The two threshold surfaces corresponding to (29) have been plotted on figure 2.
Now that the thresholds are given, only a fraction of the pseudo-bumps satisfy the inequalities at 0 and $+\infty$. In figure 3, we have plotted the subdomain of the (r_e, r_i) plane where conditions (30) are fullfilled if we impose the adequate values for θ_e and θ_i.
However, even in this subdomain pseudo-bumps are not guaranteed to be real bumps. This is illustrated on figure 4.

3.2 Stability

Now that we have been able to construct a pair of real bumps, we study their stability.
A pair of bumps is stable if and only if conditions (26) are fulfilled for all m.
The terms $h^m_{xy}(r_x)$ can be seen as Fourier coefficients. Hence they satisfy

$$\lim_{m \to +\infty} h^m_{xy}(r_x) = 0.$$

[1] $v_x(r)$ is a sum of terms of the form $b_{xy}(r, \rho) = \overline{\nu}_y \int_{D_\rho} W_{xy}(|\mathbf{r} - \mathbf{r}'|) \, d\mathbf{r}'$, where ρ, the radius of the integration domain, is fixed. As $r \to +\infty$, the terms $W_{xy}(|\mathbf{r} - \mathbf{r}'|)$ pointwise converge to 0, because W_{xy} is radially decreasing and integrable. So, in virtue of Lebesgue's theorem, each term b_{xy} converges to zero.

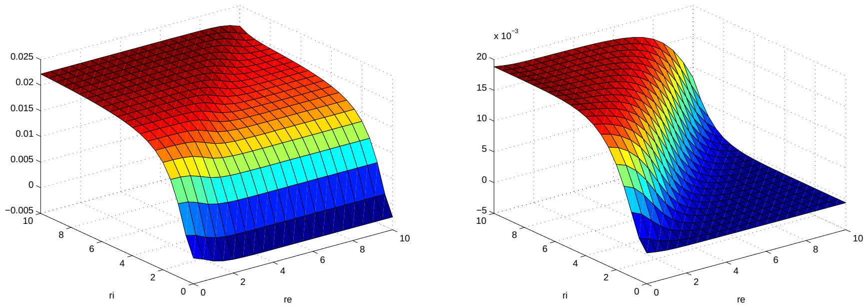

Figure 2: *Plot of* $\theta_e(r_e, r_i)$ *(left) and* $\theta_i(r_e, r_i)$ *(right).*

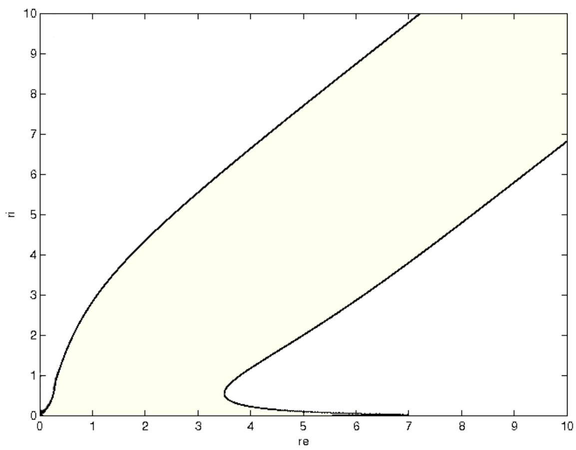

Figure 3: *Domain of the* (r_e, r_i) *plane where conditions (30) are all satisfied (light color).*

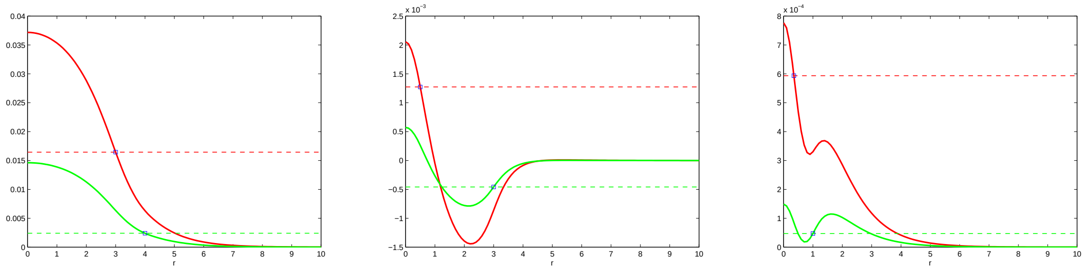

Figure 4: *Examples of pseudo-bumps profiles (solid lines, red for the excitatory layer and green for the inhibitory one) with their corresponding thresholds (dashed lines). The little blue squares indicate the points* (r_x, θ_x)*. Left. This pseudo-bumps pair is obtained for* $(r_e = 3, r_i = 4)$*, which belongs to the yellow domain in figure 3. It is actually a pair of real bumps, since it respects the global conditions (20). Middle. These pseudo-bumps are obtained for* $(r_e = 0.5, r_i = 3)$*. They do not even respect the local conditions (30), so they are not real bumps. Right. These pseudo-bumps corresponding to* $(r_e = 0.35, r_i = 1)$ *satisfy local conditions (30) but not global conditions (20), so they are not real bumps.*

So $\mathbf{M}(m) \to 0$, and we have

$$\det(\mathbf{M}(m) - \mathbf{L}) \to \frac{1}{\tau_e \tau_i} > 0 \quad \text{and} \quad \mathrm{trace}(\mathbf{M}(m) - \mathbf{L}) \to -\frac{1}{\tau_e} - \frac{1}{\tau_i} < 0.$$

So, one should particularly care about "small" values of m in the stability analysis. We show an example of stability analysis with the bump obtained for $(r_e = 3, r_i = 4)$ (see figure 4). This particular bump is not stable as can be seen on figure 5 since it will be destabilized by the isotropic component of a perturbation $(m = 0)$.
We can give an example of stable bumps. It is the case for $(r_e = 8, r_i = 8)$, as shown on figure 6.
On figure 7, we show the domain of the (r_e, r_i) plane where pseudo-bumps are stable to all perturbations (i.e. all $m \in \mathbb{N}$)[2].

4 Conclusion

In this report, we have studied some basic properties of bump solutions in a simplified neural field model. We have assumed that the field was infinite and that the wave-to-pulse transforms were Heaviside-shaped. This allowed us to use translation-invariant connectivity kernels and thanks to a right choice of these kernels, to express bump solutions in a closed form, perform a linear stability analysis on them and construct stable two-dimensional bumps.
However, those assumptions are of course unrealistic as one wants to model a part of the cortical

[2]In this particular parametrization of the neural field, it corresponds to the domain $\det(\mathbf{M}(0) - \mathbf{L}) > 0$ since all domains $\{\det(\mathbf{M}(m) - \mathbf{L}) \leq 0\}$ and $\{\mathrm{trace}(\mathbf{M}(m) - \mathbf{L}) \geq 0\}$, $m \in \mathbb{N}$ are included in $\{\det(\mathbf{M}(0) - \mathbf{L}) \leq 0\}$

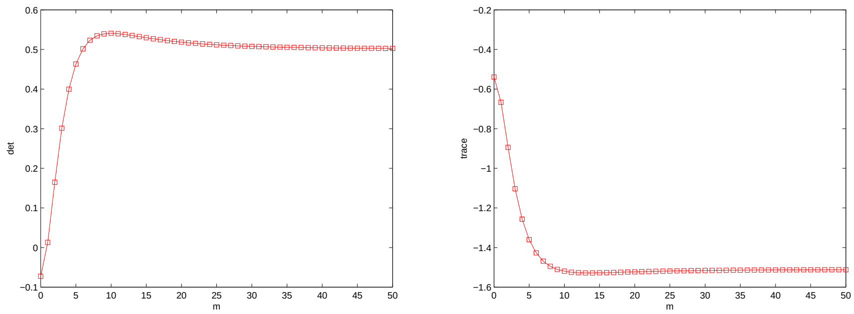

Figure 5: *Plots of the determinant (left) and trace (right) of the matrix giving stability conditions (26) for the bumps pair* $(r_e = 3, r_i = 4)$*. These bumps are not stable since the determinant is negative for* $m = 0$*.*

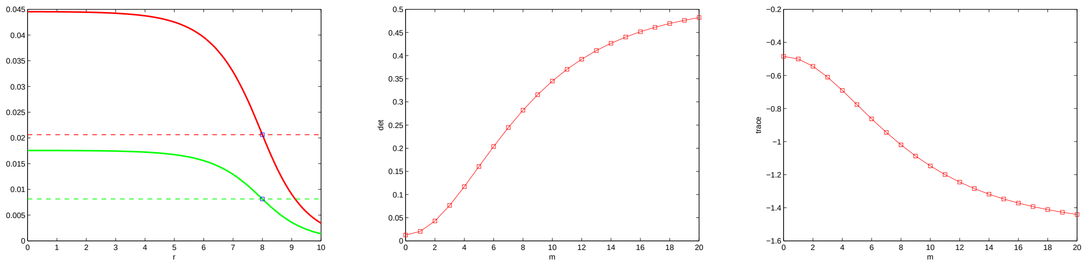

Figure 6: *Plots of the bumps profiles (left), and the determinant (center) and trace (right) of the matrix giving stability conditions for the stable bumps pair* $(r_e = 8, r_i = 8)$*.*

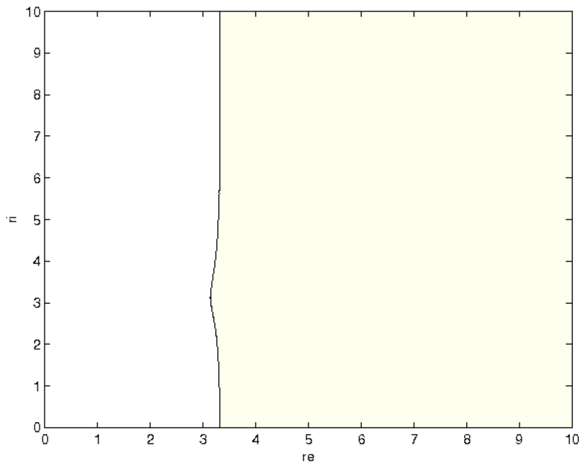

Figure 7: *Domain of the (r_e, r_i) plane where pseudo-bumps are stable to all perturbations (light color).*

tissue. In addition, the classical Cauchy problem of existence and uniqueness of solutions is ill-posed, because of discontinuities in the wave-to-pulse functions.
In the report [6], we intend to overcome these problems by proposing a more realistic neural field model defined on a compact domain and featuring Lipschitz-continuous sigmoidal transforms.

References

[1] S.-I. Amari. Dynamics of pattern formation in lateral-inhibition type neural fields. *Biological Cybernetics*, 27(2):77–87, jun 1977.

[2] S.I. Amari. Homogeneous nets of neuron-like elements. *Biological Cybernetics*, 17(4):211–220, 1975.

[3] Stephen Coombes. Waves, bumps, and patterns in neural fields theories. *Biological Cybernetics*, 93(2):91–108, 2005.

[4] P. Dayan and L. F. Abbott. *Theoretical Neuroscience : Computational and Mathematical Modeling of Neural Systems*. MIT Press, 2001.

[5] Bard Ermentrout. Neural networks as spatio-temporal pattern-forming systems. *Reports on Progress in Physics*, 61:353–430, 1998.

[6] Olivier Faugeras, François Grimbert, and Jean-Jacques Slotine. Stability and synchronization in neural fields. Technical Report RR-6212, INRIA, 2007.

[7] Stefanos E. Folias and Paul C. Bressloff. Breathing pulses in an excitatory neural network. *SIAM Journal on Applied Dynamical Systems*, 3(3):378–407, 2004.

[8] W. Gerstner and W. M. Kistler. Mathematical formulations of hebbian learning. *Biological Cybernetics*, 87:404–415, 2002.

[9] PS Goldman-Rakic. Cellular basis of working memory. *Neuron*, 14(3):477–85, 1995.

[10] J. J. Hopfield. Neurons with graded response have collective computational properties like those of two-state neurons. *Proceedings of the National Academy of Sciences, USA*, 81(10):3088–3092, 1984.

[11] H.R. Wilson and J.D. Cowan. Excitatory and inhibitory interactions in localized populations of model neurons. *Biophys. J.*, 12:1–24, 1972.

[12] H.R. Wilson and J.D. Cowan. A mathematical theory of the functional dynamics of cortical and thalamic nervous tissue. *Biological Cybernetics*, 13(2):55–80, sep 1973.

Unité de recherche INRIA Sophia Antipolis
2004, route des Lucioles - BP 93 - 06902 Sophia Antipolis Cedex (France)

Unité de recherche INRIA Futurs : Parc Club Orsay Université - ZAC des Vignes
4, rue Jacques Monod - 91893 ORSAY Cedex (France)
Unité de recherche INRIA Lorraine : LORIA, Technopôle de Nancy-Brabois - Campus scientifique
615, rue du Jardin Botanique - BP 101 - 54602 Villers-lès-Nancy Cedex (France)
Unité de recherche INRIA Rennes : IRISA, Campus universitaire de Beaulieu - 35042 Rennes Cedex (France)
Unité de recherche INRIA Rhône-Alpes : 655, avenue de l'Europe - 38334 Montbonnot Saint-Ismier (France)
Unité de recherche INRIA Rocquencourt : Domaine de Voluceau - Rocquencourt - BP 105 - 78153 Le Chesnay Cedex (France)

Éditeur
INRIA - Domaine de Voluceau - Rocquencourt, BP 105 - 78153 Le Chesnay Cedex (France)
http://www.inria.fr
ISSN 0249-6399